

# Clinical Case Report: Renal Ewing Sarcoma in Pregnant Patient: Magnetic Resonance Imaging Approach and Bibliographical Review

Alejandro Manuel Bolón Ojeda, Vania Paola Balcazar Vidal, Jhonatan Gómez Domínguez

Department of Radiology and Imaging, Juan Graham Casassus Hospital, Villahermosa City, Mexico

Email: jhonatangomdom@gmail.com

**How to cite this paper:** Bolón Ojeda, A.M., Balcazar Vidal, V.P. and Gómez Domínguez, J. (2024) Clinical Case Report: Renal Ewing Sarcoma in Pregnant Patient: Magnetic Resonance Imaging Approach and Bibliographical Review. *Open Journal of Urology*, 14, 562-571.

<https://doi.org/10.4236/oju.2024.1411059>

**Received:** September 27, 2024

**Accepted:** November 23, 2024

**Published:** November 26, 2024

Copyright © 2024 by author(s) and Scientific Research Publishing Inc.

This work is licensed under the Creative Commons Attribution International License (CC BY 4.0).

<http://creativecommons.org/licenses/by/4.0/>



Open Access

## Abstract

The case report presents the clinical case of a pregnant patient with renal Ewing's sarcoma, an extremely rare tumor. Renal tumors during pregnancy are uncommon, with renal cell carcinoma being the most frequent. The diagnosis of cancer during pregnancy has increased due to the use of non-invasive prenatal testing (NIPT) and advanced maternal age. Renal tumors, such as Ewing's sarcoma, present a diagnostic and therapeutic challenge due to the physiological changes during pregnancy. Renal Ewing's sarcoma is aggressive and tends to manifest with abdominal pain, a palpable mass, and severe hematuria. However, its symptoms often go unnoticed, leading to late diagnosis with distant metastasis and poor prognosis. This type of tumor is diagnosed through histopathological studies, as imaging alone is insufficient for its characterization. In the presented case, multiparametric magnetic resonance imaging (MP-MRI) was used to assess the renal mass due to the limitations of using computed tomography in pregnant women. MRI provides both morphological and behavioral information about the tumor and is particularly useful in patients where radiation exposure is contraindicated. In this case, the MRI revealed a large tumor in the left kidney, with extension to adjacent structures, thrombosis in the vena cava, and hepatic and bone metastases. The article concludes that this is the largest renal Ewing's sarcoma tumor described in a pregnant patient in the literature. It highlights the importance of early diagnosis and appropriate intervention to improve the prognosis in these rare but aggressive cases.

## Keywords

Pregnancy, Tumors Renal, Ewing's Sarcoma

## 1. Introduction

Pregnancy-related cancer is that neoplastic process which is detected during the pregnancy and up to one year after childbirth. Currently, there has been an increase in cancer diagnosis during pregnancy due to the tendency of advanced maternal age, as well as the rise in incidental findings because of the use of noninvasive prenatal testing (NIPT) in the search of fetal aneuploidies. Some hypotheses state there is a high estrogen production, an augment in the production of angiogenesis by the placenta, and immunosuppression during pregnancy, which increases the risk of having cancer during gestation. The interpretation of diagnosis image methods and staging in pregnant women with cancer represent a challenge due to physiological changes [1]. Among the most common neoplasias during pregnancy are breast cancer (41%), lymphoma (14%), cervical cancer (10%), leukemia (8%), and ovary tumors (22%) [2].

Renal tumors are seldom found during pregnancy, being the renal cell carcinoma the most frequent gestational renal tumor. It appears with mass and pain in abdominal flank, hematuria, fever, abdominal distension and hypertension; hemolytic anemia, hypercalcemia, and tumor rupture cases are among other less frequent symptoms. Regardless the primary or secondary etiology nature of renal tumors, they become a real challenge for their diagnosis and treatment during pregnancy. In addition, it is necessary to take the risk factors which can condition renal cancer during gestation into consideration. Among the most important risk factors are obesity, tobacco consumption, analgesics use, hypertension, diabetes, chronic renal disease, and hormone medicine use. Also, it has been noticed a risk of renal cancer in multiparous patients (more than 5 pregnancies) [3] [4].

Ewing's Sarcoma (ES), also known as Primitive Neuroectodermal Tumor (PNET) in kidney was first described by Seemaver and colleagues in 1975. It represents 1% of all renal tumors with scarce literature and scarce case reports. Tumors with a clinical aggressive behavior often appear between 20s and 30s, being slightly more common in women. Renal ES tumors often present the typical abdominal pain triad, palpable mass, and severe hematuria. Nevertheless, ES tends to hide its symptoms given its high malignant nature, which results in a distant metastasis diagnosis with a poor prognosis. Given the scarcity of clinical cases of renal ES, its diagnosis means a real challenge, in addition to the inconsistent proper handling. The final diagnosis is made through histopathology, since it is almost impossible to characterize the histological strain of kidney tumors by imaging methods [5]-[7]. As far as it is known, the case that is going to be described next is the biggest renal tumor ever found in a pregnant patient in literature.

The objective of the presented clinical case is to document a rare case of renal Ewing's sarcoma in a pregnant patient, emphasizing the diagnostic and therapeutic challenges that this type of tumor poses during pregnancy. It aims to highlight the importance of early diagnosis and the use of non-invasive imaging techniques, such as multiparametric magnetic resonance imaging (MP-MRI), to improve the prognosis in patients diagnosed with this aggressive tumor, as well as to raise

awareness about the incidence of renal tumors during pregnancy, in a context where advances in prenatal testing and the increasing maternal age have contributed to more frequent cancer diagnoses in pregnant women.

## **2. The Multi-Parametric Magnetic Resonance Imaging (MRI)**

MRI represents a valuable imaging technique which is a complement for the renal masses assessment, giving morphologic information as well as information related to their behavior because of the sequences. Its use is mainly recommended when a computerized CT scan cannot be done (whether it happens because of a severe allergy caused by iodine with contrast medium, or the high risk of induced nephropathy with contrast medium), or when radiation exposure is contraindicated (whether it is because of an early age or pregnant women).

Both 1,5-T and 3-T magnetic resonance imaging systems can be used to obtain images during pregnancy. Animal simulation studies and computerized studies have proven fetal tissues heating it is not significant, particularly to a 1,5 T field force [2].

Renal magnetic resonance imaging protocol comprehends the following sequences: T1-weighted imaging (in phase and out of phase), also known as DIXON technique, T2-weighted imaging, diffusion weighted imaging (DWI), T1-weighted contrast-enhanced dynamic subtraction images in early and late arterial phase.

Clear-cell renal cell carcinoma (RCC) is the most frequent malignant tumor in the urinary system in pregnant women. It often appears in large sizes and is heterogeneous, with an increase of the signal intensity in T2 and ADC; as well as an avid heterogeneous rise in an early phase after the contrast agent is administrated.

Magnetic resonance imaging provides additional information in cases where there have been indetermined TC injuries, especially when the perinephric fat infiltration is assessed, as well as the casing and vascular extension [8].

Variables of RCC sarcomatoid show high degree transformation signs without being a different histological entity, and they are the most frequent ill-defined and infiltrative injuries in the images [9] [10].

## **3. Non-Contrast-Enhanced Magnetic Resonance Imaging Acquisitions for Hepatic Metastasis Assessment**

In-phase and Out-of-phase T1: they are gradient echo sequences (GRE) which are prone to susceptibility and to chemical shift artifacts. This property can be used to detect and quantify the iron deposition and fat inside the liver parenchyma, or in focal lesions. Chemical shift artifacts are caused by the differences in the precession frequency of fat and water protons. This creates coherence in the periodic phase where voxel signals are the sum or the opposition of water and fat signals. These differences allow the detection of intracellular fat in hepatic lesions or in the hepatic parenchyma [11].

Fast spin-echo sequences or T2 turbo spin-echo, with or without fat suppressed imaging: they are rather fast sequences; currently, they can also be acquired

through the breath-holding technique. They are known for having a 90° pulse followed by various 180° refocusing pulses to fill several K-space lines (echo train) during a repetition period. The contents of the liquid are the predominant information obtained from this type of sequences, which permits the discrimination between solid and cystic focal lesions. Fat-suppressed imaging must be used regularly to increase contrast resolution.

Diffusion weighted imaging (DWI) are T2-weighted images obtained with only one taking and echo-planar imaging techniques. Several series of diffusion weighted imaging are obtained modifying the gradient strength and the magnitude (b-value). It is important to acquire a series with a 0 b-value to be able to gather similar information to fat sequences. Other series must be taken with increasing b-values (b50, b400, b800) to detect secondary lesions, provided black-blood increases notability of lesions located next to the vessels. Series with a high b-value (b800) are essential to determine hepatic lesions, due to the fact that highly cellular tissues, such as metastasis, show a diffusion restriction, which makes them hyperintense in DWI. Diffusion weighted sequences have a high spatial resolution, and they are useful to study the movement of water molecules in the tissue in a microscopic level [12].

#### **4. Weighted Acquisitions in Magnetic Resonance Imaging to Assess Hepatic Metastasis**

The gadolinium-based contrast agent is category C during pregnancy with adverse effects. Therefore, DWI can be used as an alternative to gadolinium. Small solid renal masses in kidney limit water diffusion (DWI) and decrease the Apparent Diffusion Coefficient (ADC) value, which makes them seem hypointense in ADC maps [2].

Hepatic metastases show characteristics of lesions in the form of a target in T2 sequences, which are an indicative of hypovascular metastases, being the adenocarcinoma the most common cause. In T1 and T2 sequences, the central area of the lesions appears as hypointensity, which suggests the presence of fibrous shift or old hemorrhage. Moreover, in cases in which there is liquefactive necrosis or cystic degeneration it is possible to observe hyperintensity areas in T2-weighted images, and a mild hyperintensity in T1-weighted images. The histopathologic contrast between the central and peripheral areas is visualized as the characteristic sign in target.

On the other hand, there are hypervascular metastases which tend to be more common in renal, thyroid, hepatocellular, and melanoma primary tumors. These metastases can be observed with hypo in moderated hyperintensity in T1 and T2 sequences respectively. Metastases that are observed in a hyperintense way in T1 suggest a melanoma primary. Hypervascular metastases can only be observed with contrast agents [13].

#### **5. Acquisitions in Magnetic Resonance Imaging to Assess Bone Tissue Metastasis**

Due to its high contrast between soft tissues and the spatial resolution, the MRI

can detect bone tissue metastasis with a 91% accuracy, and 95% specificity even in early stages, before changes can be distinguished by a CT scan in bone mass [14].

The second commonest place for kidney tumor spreading is to bone tissue structures. In comparison among other malignancies, the distribution of bone tissue metastases varies and has the pelvis, the spine, and ribs as the most common places.

Using T1-weighted sequences, Short tau inversion recovery (STIR) and Diffusion weighted imaging with ADC mapping, it has been proved that magnetic resonance imaging is more sensitive and specific than the bone gammagraphy. There are focal or diffused areas of hypointensity shown in T1; in the STIR sequence, lesions are hyperintense [15].

## 6. Clinical Case Report

In the following lines, it is described the case of a 23-year-old female patient, with a 17.2 weeks of gestation pregnancy in her third gestation, with alcohol, tobacco, and cocaine consumption records. She states she stopped consuming them two years ago. The patient arrives to the emergency room showing pelvic pain, nausea, vomit, and orthopnea, without any other symptoms. During physical examination it is detected a globose abdomen due to gestating uterus and a painful, indurated, fixed tumor with asymmetrical and irregular edges on the left side. An abdominal echography is performed where the following important findings are shown: left kidney with morphology loss, with an augmented size in a generalized form with  $237 \times 147 \times 185$  mm dimensions in their greatest axes, indefinite edges, heterogeneous parenchyma with areas of greater or smaller echogenicity, there is a loss of the marrow cortex relation which conditions the movement of intra-abdominal adjacent structures. In addition, it is identified in the inferior vena cava an echogenic image which partially obstructs its light, with a segmental absence of the Doppler color flow. This is non-compressible to the transduce in relation with thrombosis (**Figure 1**). Subsequently, a MRI is performed, recommended by the radiologist, where it can be observed that the left kidney has a morphology loss caused by a major irregular heterogeneous lesion, T1 hypointense and T2 mixed sign intensity, as well as solid-predominant T2 FAT-SAT with an ill-defined high intensity center in relation to cystic degeneration VS necrosis. Additionally, there is a peripheral-predominant DWI restriction. The lesion has an extension of  $186 \times 177$  mm in its axial axes (**Figure 2**). There are nodular images with a random distribution in the mesentery and parietal peritoneum. The biggest image is 36 mm in size which are compatibles with implants. In addition to this, a thrombosis in the vena cava was found, which was described using an echography (**Figure 3**). The liver and bone structures with lesions compatible with metastasis were shown (**Figure 4** and **Figure 5**).

After conducting the appropriate imaging studies, it was determined that a biopsy of the tumor in the left kidney was necessary, which would be carried out

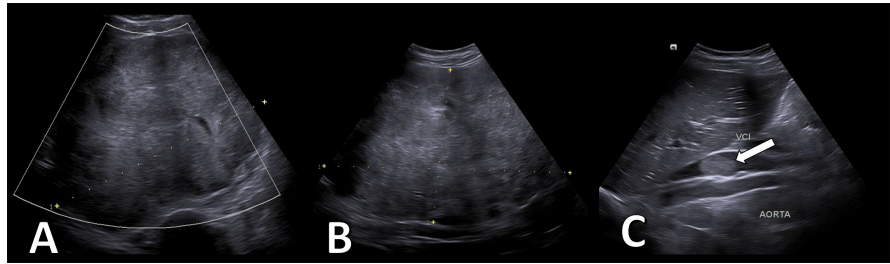


**Figure 1.** Echography images with a high frequency convex transducer in topography of the left renal fossa (A) and (B) where a great lesion with irregular morphology can be seen, as well as undefined and heterogeneous edges at the expense of ill-defined zones of greater and smaller echogenicity. (C) In the inferior vena cava the presence of an image with ovoid morphology, circumscribed margins, and echogenic, with an endoluminal localization related to thrombosis (white arrow).

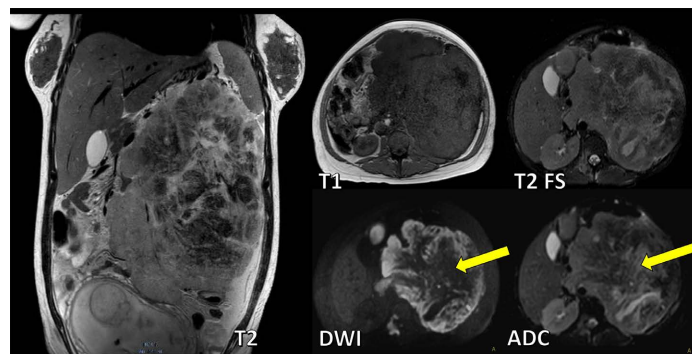


**Figure 2.** Magnetic resonance images in axial and coronal plane show the left kidney with a morphology change due to a great tumoral lesion with irregular and undefined margins. This lesion affects the interface with adjacent structures. It is hypointense in the T1 sequence, while in the fluid sensitive sequences (T2 and T2 FS) it shows a heterogeneous sequence with isointense predominance, together with a center with irregular and ill-defined increase because of the signal intensity that suggests the existence of necrosis or cystic degeneration. In DWI, it can be seen an irregular peripheral restriction with a loss of signal in ADC, and the lesion center appears to be hypointense in DWI, and heterogeneous in ADC (yellow arrow).

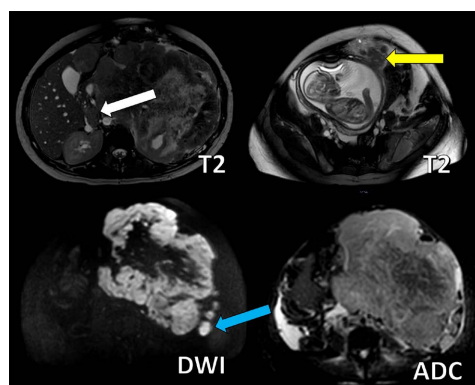


**Figure 3.** T2-weighted turbo spin-echo sequences and DWI magnetic resonance images in axial plane with a thrombosis presence in the inferior vena cava (white arrow), as well as peritoneal implants (yellow arrow). In DWI sequences, adenopathies in the peripheral area of the renal lesion can be observed (blue arrow).

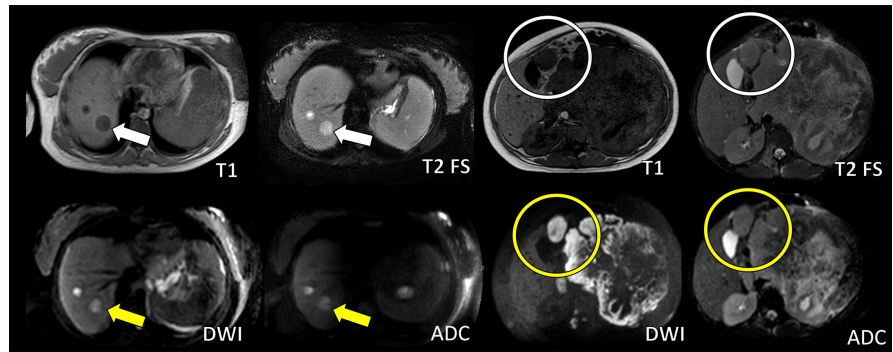


**Figure 4.** Magnetic resonance images with acquisitions in different axial pulse sequences where, at the Couinaud segment 7 of the hepatic gland, circumscribed lesions with round morphology, hypointense in T1, and hyperintense in T2 FS (white arrows) are observed. They are associated with a focal restriction on DWI, and they have an increase in the signal intensity in ADC (yellow arrows). Besides the topography of the 4b segment, there is a circumscribed focal lesion with an ovoid morphology, which is hypointense in T1 sequence, and isointense to the parenchyma in T2 FS (white circles). This lesion has a restriction in DWI with a signal loss in ADC (yellow circles).

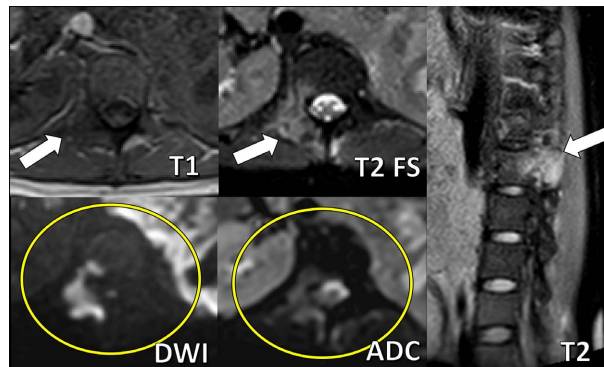


**Figure 5.** Magnetic resonance images obtained in an axial and sagittal plane where an ill-defined lesion with irregular morphology in the posterior wall of the vertebral body L1 with pedicle involvement and right neural foramen can be distinguished (white arrow). In addition to this, it is shown with a restriction on DWI (yellow circle).

by the interventional radiology department of our hospital. An ultrasound examination of the abdomen was performed, where a mass occupying almost the entirety of this cavity was identified. It was decided to proceed with the approach to the lesion in the hypogastric region. Proper aseptic preparation was carried out, sterile fields were placed, and the area was infiltrated with a solution of lidocaine combined with epinephrine. Subsequently, a 16 G, 16 cm needle was introduced, and five tissue cylinders were obtained. The procedure was carried out without complications.

Histopathological result with a positive report for CD45, CD99, FLI-1, and WT-1, specific to Ewing's sarcoma.

A uterine instrumental curettage was performed for the termination of the pregnancy. Subsequently, a chemotherapy treatment was initiated that included vincristine, doxorubicin, and cyclophosphamide, completing a total of six cycles to

date. Currently, the patient is under the care of a palliative care team, where pain management is provided through buprenorphine patches, with no other medical or surgical treatment available to offer at this time.

## 7. Discussion

The trend of starting pregnancy at an older age is a significant risk factor for cancer during pregnancy. In the case of kidney tumors, there is often a delay in diagnosis as the symptoms can be very similar to those of other urinary tract diseases that may occur during pregnancy. However, the diagnosed renal cancer suspicion must be considered in case a pregnant woman has symptoms of a recurrent urinary tract disease, or immune to a treatment, palpable mass and renal pain [16] [17].

The standard imaging modality for detecting renal masses is multiphase CT of the kidneys, but it is contraindicated in pregnant patients. Alternatives such as ultrasound and MRI are considered. The guidelines from the Royal Australian and New Zealand College of Radiologists indicate a theoretical risk of teratogenesis due to exposure to electromagnetic fields during the first trimester, as well as possible concerns about fetal hearing and thermal stress. However, follow-up studies have shown that children exposed to scans in different trimesters do not exhibit harmful effects [6]. Through imaging methods RCC and renal ES are similar. In fact, all solid renal tumors identified during pregnancy should be considered as RCC unless proven otherwise [3].

The renal ES is an extremely rare disease with scarce reported cases. Its unusual therapeutic approach presentation tends to be unspecified, and it has a poor prognosis with a survival rate up to 5 years of 45% - 55%. The recurrence rate in patients who receive local treatment is greater than 80%. Furthermore, due to its high degree of malignancy and its fast growth at the moment of the diagnostic approach they tend to have locoregional and distant metastases. Most frequent metastases affect lungs, liver, and bones. The definite diagnosis is done through histopathology and immunohistochemistry. They often show small round cells with a relatively uniform size. They also show preserved nuclear chromatin, as well as round cells with a rosette pattern, and they are positive to CD99, FLI-1, and SYN during immunohistochemical staining [5] [18].

Due to the existing risks to exposing the fetus to radiation during the CT, as well as the use of intravenous contrast agents, the echography and MRI are really useful when there is a suspicion of renal tumors, even during the initial staging [19].

To the best of our knowledge, this article talks about the biggest primary renal ES tumor in a pregnant woman ever described in literature. Moreover, there were descriptions of compatible images, peritoneal implants, hepatic lesions, and bone lesions using magnetic resonance imaging in relation to metastasis. The most useful sequence to use in case of acquisition in simple phase is DWI, which has a sensitivity and specificity of 95% to distinguish between benign and malignant

lesions [20] [21].

It is expected that the information shown in this article be of great usefulness in the clinical and radiology areas to identify future ES with a renal origin.

## 8. Conclusion

Renal ES is extremely rare, and its definite diagnostic is done through histopathology. Given that renal ES has a high degree of malignancy with a fast growth and poor prognosis, a timely diagnostic is crucial to intervene with an adequate handling, so a promising result is achieved. Radiologists must recognize and interpret malignancy characteristics through imaging methods, thus recognizing locoregional and distant metastases, which allows an adequate staging for prognosis and medical handling of the patient.

## Conflicts of Interest

The authors declare no conflicts of interest regarding the publication of this paper.

## References

- [1] Vandecaveye, V., Amant, F., Lecouvet, F., Van Calsteren, K. and Dresen, R.C. (2021) Imaging Modalities in Pregnant Cancer Patients. *International Journal of Gynecologic Cancer*, **31**, 423-431. <https://doi.org/10.1136/ijgc-2020-001779>
- [2] Jha, P., Pöder, L., Glanc, P., Patel-Lippmann, K., McGettigan, M., Moshiri, M., *et al.* (2022) Imaging Cancer in Pregnancy. *Radio Graphics*, **42**, 1494-1513. <https://doi.org/10.1148/rg.220005>
- [3] Ghorbani, H., Mottaghi, M. and Soltani, S. (2022) Renal Tumors in Pregnancy: A Case Report Focusing on the Timing of the Surgery and Patient Positioning. *Case Reports in Obstetrics and Gynecology*, **2022**, 1-4. <https://doi.org/10.1155/2022/1143478>
- [4] Ding, X., Xu, J., Zhou, J. and Long, Q. (2020) Chest CT Findings of COVID-19 Pneumonia by Duration of Symptoms. *European Journal of Radiology*, **127**, Article 109009. <https://doi.org/10.1016/j.ejrad.2020.109009>
- [5] Zhang, S., Li, Y., Wang, R. and Song, B. (2019) Ewing's Sarcoma/Primitive Neuroectodermal Tumor of the Kidney: A Case Report and Literature Review. *Translational Andrology and Urology*, **8**, 562-566. <https://doi.org/10.21037/tau.2019.09.46>
- [6] Bray, G., Nesbitt, A., Maré, A., Willis, T. and Tracey, C. (2023) Primary Ewing Sarcoma of the Kidney Presenting as Haematuria in a Pregnant Woman—A Case Report Highlighting the Diagnostic and Therapeutic Dilemmas of the Condition in Pregnancy. *Urology Case Reports*, **46**, Article 102308. <https://doi.org/10.1016/j.eucr.2022.102308>
- [7] Lai, T., Lin, Y. and Yang, M. (2021) Primary Ewing Sarcoma of the Kidney with Inferior Vena Cava and Right Atrial Tumor Thrombi Successfully Treated with Two-Stage Surgery. *Asian Journal of Surgery*, **44**, 757-758. <https://doi.org/10.1016/j.asjsur.2021.02.001>
- [8] Papalia, R., Panebianco, V., Mastroianni, R., Del Monte, M., Altobelli, E., Faiella, E., *et al.* (2019) Accuracy of Magnetic Resonance Imaging to Identify Pseudocapsule Invasion in Renal Tumors. *World Journal of Urology*, **38**, 407-415. <https://doi.org/10.1007/s00345-019-02755-1>

- [9] Rubin, G.D., Ryerson, C.J., Haramati, L.B., Sverzellati, N., Kanne, J.P., Raoof, S., *et al.* (2020) The Role of Chest Imaging in Patient Management during the COVID-19 Pandemic. *Chest*, **158**, 106-116. <https://doi.org/10.1016/j.chest.2020.04.003>
- [10] Ljungberg, B., Albiges, L., Abu-Ghanem, Y., Bensalah, K., Dabestani, S., Fernández-Pello, S., *et al.* (2019) European Association of Urology Guidelines on Renal Cell Carcinoma: The 2019 Update. *European Urology*, **75**, 799-810. <https://doi.org/10.1016/j.eururo.2019.02.011>
- [11] Maino, C., Vernuccio, F., Cannella, R., Cortese, F., Franco, P.N., Gaetani, C., *et al.* (2023) Liver Metastases: The Role of Magnetic Resonance Imaging. *World Journal of Gastroenterology*, **29**, 5180-5197. <https://doi.org/10.3748/wjg.v29.i36.5180>
- [12] De Perrot, T., Sadjo Zoua, C., Glessgen, C.G., Botsikas, D., Berchtold, L., Salomir, R., *et al.* (2022) Diffusion-Weighted MRI in the Genitourinary System. *Journal of Clinical Medicine*, **11**, Article 1921. <https://doi.org/10.3390/jcm11071921>
- [13] Ozaki, K., Higuchi, S., Kimura, H. and Gabata, T. (2022) Liver Metastases: Correlation between Imaging Features and Pathomolecular Environments. *Radio Graphics*, **42**, 1994-2013. <https://doi.org/10.1148/rg.220056>
- [14] Mansinho, A., Nejo, P., Leitão, T., Casimiro, S. and Costa, L. (2021) Management of Bone Metastases in Renal Cell Carcinoma: Bone-Targeted Treatments, Systemic Therapies, and Radiotherapy. *Journal of Cancer Metastasis and Treatment*, **7**, Article 44. <https://doi.org/10.20517/2394-4722.2021.88>
- [15] Griffin, N., Gore, M.E. and Sohaib, S.A. (2007) Imaging in Metastatic Renal Cell Carcinoma. *American Journal of Roentgenology*, **189**, 360-370. <https://doi.org/10.2214/ajr.07.2077>
- [16] Khaled, H., Lahloubi, N.A. and Rashad, N. (2016) Review on Renal Cell Carcinoma and Pregnancy: A Challenging Situation. *Journal of Advanced Research*, **7**, 575-580. <https://doi.org/10.1016/j.jare.2016.03.007>
- [17] Scavuzzo, A., Santana Rios, Z., Diaz-Gomez, C., Varguez Gonzalez, B., Osornio-Sanchez, V., Bravo-Castro, E., *et al.* (2017) Renal Cell Carcinoma in a Pregnant Woman with Horseshoe Kidney. *Urology Case Reports*, **13**, 58-60. <https://doi.org/10.1016/j.eucr.2015.11.004>
- [18] Goud, E.R., Srikanth, J., *et al.* (2019) Primary Ewing's Sarcoma of Kidney—A Rare Case Report. *IOSR Journal of Dental and Medical Sciences*, **18**, 24-27.
- [19] Gui, B., Cambi, F., Micco, M., Sbarra, M., Petta, F., Autorino, R., *et al.* (2020) MRI in Pregnant Patients with Suspected Abdominal and Pelvic Cancer: A Practical Guide for Radiologists. *Diagnostic and Interventional Radiology*, **26**, 183-192. <https://doi.org/10.5152/dir.2019.19343>
- [20] Geneidi, E.A.S., Ali, H.I. and Dola, E.F. (2016) Role of DWI in Characterization of Bone Tumors. *The Egyptian Journal of Radiology and Nuclear Medicine*, **47**, 919-927. <https://doi.org/10.1016/j.ejrn.2016.06.017>
- [21] Bozgeyik, Z., Onur, M.R. and Poyraz, A.K. (2013) The Role of Diffusion Weighted Magnetic Resonance Imaging in Oncologic Settings. *Quantitative Imaging in Medicine and Surgery*, **3**, 269-278. <https://doi.org/10.3978/j.issn.2223-4292.2013.10.07>